Analyst

This is an *Accepted Manuscript*, which has been through the Royal Society of Chemistry peer review process and has been accepted for publication.

Accepted Manuscripts are published online shortly after acceptance, before technical editing, formatting and proof reading. Using this free service, authors can make their results available to the community, in citable form, before we publish the edited article. We will replace this *Accepted Manuscript* with the edited and formatted *Advance Article* as soon as it is available.

You can find more information about *Accepted Manuscripts* in the **Information for Authors**.

Please note that technical editing may introduce minor changes to the text and/or graphics, which may alter content. The journal's standard **Terms & Conditions** and the **Ethical guidelines** still apply. In no event shall the Royal Society of Chemistry be held responsible for any errors or omissions in this *Accepted Manuscript* or any consequences arising from the use of any information it contains.

Journal Name

ARTICLE

Grating coupled SPR microarray analysis of proteins and cells in blood from mice with breast cancer

A. Mendoza,[a] D.M. Torrisi,[a] S. Sell,[a] N.C. Cady,[b] and D.A. Lawrence[a]

Biomarker discovery for early disease diagnosis is highly important. Of late, much effort has been made to analyze complex biological fluids in an effort to develop new markers specific for different cancer types. Recent advancements in label-free technologies such as surface plasmon resonance (SPR)-based biosensors have shown promise as a diagnostic tool since there is no need for labeling or separation of cells. Furthermore, SPR can provide rapid, real-time detection of antigens from biological samples since SPR is highly sensitive to changes in surface-associated molecular and cellular interactions. Herein, we report a lab-on-a-chip microarray biosensor that utilizes grating-coupled surface plasmon resonance (GCSPR) and grating-coupled surface plasmon coupled fluorescence (GCSPCF) imaging to detect circulating tumor cells (CTCs) from a mouse model (FVB-MMTV-PyVT). GCSPR and GCSPCF analysis was accomplished by spotting antibodies to surface cell markers, cytokines and stress proteins on a nanofabricated GCSPR microchip and screening blood samples from FVB control mice or FVB-MMTV-PyVT mice with developing mammary carcinomas. A transgenic MMTV-PyVT mouse derived cancer cell line was also analyzed. The analyses indicated that CD24, CD44, CD326, CD133 and CD49b were expressed in both cell lines and in blood from MMTV-PyVT mice. Furthermore, cytokines such as IL-6, IL-10 and TNF-⍰, along with heat shock proteins HSP60, HSP27, HSc70(HSP73), HSP90 total, HSP70/HSc70, HSP90, HSP70, HSP90 alpha, phosphotyrosine and HSF-1 were overexpressed in MMTV-PyVT mice.

Introduction

Molecular characterization of circulating tumor cells (CTCs)[1], as well as their detection[2], capture[3], 3D filtration[4], and biomarker discovery[5, 6], is an emerging focus for cancer research. To date, most research regarding breast cancer has emerged from *in vitro* studies with mouse and/or human tumor cell lines to use of transgenic models to assess the status of CTCs *in vivo*; the FVB/N-MMTV-PyVT transgenic mouse model[7] is such a model. This FVB strain has been genetically altered to enhance early development of adenocarcinomas for evaluation of tumor progression[8]. The number of blood CTCs increase as the disease progresses. Thus, early detection of CTCs, which are rare and hard to detect, can be readily followed along with plasma protein and circulating leukocyte changes as cancer progression occurs.

Thus far, clinical analysis of blood from patients has been expensive, laborious, reagent intensive (requiring extensive sample preparation), or limited by poor detection methods. The CellSearch system (Veridex, Warren, NJ) is the current state-of-the-art FDA-approved technology for quantification of CTCs. This system is designed to enrich and enumerate circulating tumor cells (CTCs) from peripheral blood, but it is limited to the analysis of an isolated subset based on a single surface marker, and it does not assess any other cells and proteins in the blood. However, the CellSearch system was reported to provide prognostic values when the CTC levels of breast cancer patients were ≥ 5 CTCs per 7.5 ml of whole blood[9]. There continues to be a need for an inexpensive platform with analytical multiplexed cellular and molecular capacity of biomarkers that permits sensitive, quantitative, rapid, labeled and label-free detection, as well as detection of multiple analytes (bacteria, viruses, proteins, DNA and mammalian cells) from both clinical and environmental samples in a single assay. More importantly, the ability to detect low concentrations of CTCs from blood, at the same time as quantification of immune potential, would be ideal for the early stage diagnosis and prognosis of and therapeutic response to cancers such as breast cancer.

Among women, breast cancer is the second leading cause of death and the most commonly diagnosed cancer in the USA[10]. Worldwide, it is the most common type of cancer claiming the lives of hundreds of thousands of residents in numerous countries[11]. The costs associated with breast cancer care reach into the billions of dollars in the USA alone[10]. The potential prognostic and diagnostic capacity of a dual-mode microfluidic SPR instrument based on grating-coupled surface plasmon resonance (GCSPR) and grating-coupled surface plasmon coupled fluorescence (GCSPCF) imaging[12, 13] could

a. Wadsworth Center, New York State Department of Health, 150 New Scotland Avenue, Albany, NY 12208, USA
b. SUNY Polytechnic Institute, 257 Fuller Road, Albany, NY 12203, USA.

improve diagnosis and potential treatment strategies, thereby reducing the costs associated with breast cancer care. In this study, a broad range of biomarkers consistent with breast cancer cell phenotypes were immobilized onto a gold-coated microchip using a robotic contact pin spotter. A unique grating-based SPR instrument (Ciencia, Inc) was used. This instrument possesses the ability to detect analytes and ligand interactions utilizing a microchip, 1 cm^2, which can accommodate 1024 spots or regions of interest (ROIs), as previously described[12, 13]. The GCSPR instrument utilizes a label-free microarray platform that can assess real-time mass changes at a metal/dielectric interface with high sensitivity (µg/ml), however, it also incorporates grating-coupled surface plasmon coupled fluorescence (GCSPCF) in which fluorescent dye labeling (secondary reagent conjugated to Alexa Fluor 647 or labeled cells) dramatically increases the assay sensitivity (pg-ng/ml). Sensitivity and specificity are critical aspects for diagnosis and prognosis. The instrument can simultaneously measure multiple antigen-antibody interactions, which can be used to assess immune or physiological changes due to the onset of cancer. Thus, the ability to capture a wide range of analytes from blood can delineate unique bio-signatures providing a holistic approach used to develop characteristics of developing cancer and/or host-cancer interactions.

Herein we report a microarray method based on GCSPR and GCSPCF imaging for detecting circulating tumor cells (CTCs) and various analytes in blood from FVB/N-MMTV-PyVT (MMTV) mice. The aim was to optimize conditions for screening blood from control FVB/NJ mice and MMTV mice with a set of antibodies to cell surface markers that can identify and capture breast cancer cells or the 419 mouse tumor cell line. The 419 tumor cells used in this study are cancer cells derived from a transgenic MMTV-PyVT mouse[14, 15]. MMTV-polyomavirus middle T antigen (MMTV-PyVT) transgenic mice[7] are an inbred strain of genetically modified mice commonly used in research because of their ability to develop mammary carcinomas, which mimics the development of breast cancer in humans. FVB/NJ mice, on the other hand, are the genetic background inbred strain of mice used as the control strain.

Materials & Methods

Materials
Gold-coated GCSPR biosensor microchips, 1 cm^2, were fabricated at the SUNY Polytechnic Institute's Colleges of Nanoscale Sciences and Engineering (Albany, NY). The ligands, proteins and antibodies pin spotted on each microchip included bovine serum albumin (BSA, Sigma-Aldrich), anti-mCD178 (BD Pharmingen), anti-mCD5 (BD Pharmingen), anti-mEarly Activation Marker (PharMingen), anti-mCD80 (BD Pharmingen), anti-mCD38 (BD Pharmingen), Mac-3 (PharMingen), anti-mCD28 (BD Pharmingen), anti-mCD23 (BD Pharmingen), anti-mCD44 (BD Pharmingen), anti-mCD11a (BD Pharmingen), anti-mCD26 (BD Pharmingen), anti-mCXCL12/SDF-1 (R&D Systems), anti-mCXCR4 (R&D Systems),

Rat IgG (BD Pharmingen), anti-mCD197 (eBioscience), hamster IgG (BD Pharmingen), anti-mGFAP (BD Pharmingen), anti-mCD24 (BD Pharmingen), anti-mCD133 (eBioscience), anti-mCD3e (BD Pharmingen), anti-mCD19 (eBioscience), anti-mCD11b (BD Pharmingen), anti-mCD45 (BD Pharmingen), anti-mCD106 (BD Pharmingen), FoxP3 (BD Pharmingen), Annexin-V (BD Pharmingen), anti-mCD11c (BD Pharmingen), anti-mCD326 (BD Pharmingen), anti-mCD152 (BD Pharmingen), anti-mCD8 (BD Pharmingen), anti-mCD40 (BD Pharmingen), anti-mCD8 beta-chain (BD Pharmingen), anti-mIgE (Southern Biotech), anti-mCD273, anti-mIgG (Southern Biotech), anti-mIFN gamma (BD Pharmingen), anti-mTNF alpha (BD Pharmingen), anti-mCD28 (BD Pharmingen), anti-mIL-10 (BD Pharmingen), anti-mIL-12 (BD Pharmingen), anti-mToll Like Receptor 2 (eBioscience), anti-mCD25 (BD Pharmingen), anti-mCD49f (eBioscience), anti-mCD54 (BD Pharmingen), anti-mCD4 (BD Pharmingen), anti-mCD123 (BD Pharmingen), anti-mCD138 (BD Pharmingen), anti-mCD14 (BD Pharmingen), anti-mCD71 (BD Pharmingen), anti-mCD62L (BD Pharmingen), anti-mCD117 (BD Pharmingen), anti-mCD31 (BD Pharmingen), anti-mCD34 (BD Pharmingen), anti-mCD90.2 (BD Pharmingen), anti-mIL-6 (BD Pharmingen), anti-mCD86 (BD Pharmingen), anti-mCD83 (BD Pharmingen), anti-mVβ 9 T-Cell Receptor (BD Pharmingen), anti-mCD49b (BD Pharmingen), anti-mCD184 (BD Pharmingen), anti-mCD69 (PharMingen), anti-mCD127 (BD Pharmingen), anti-mGamma II Receptor (BD Pharmingen), anti-mHSP60 (StressMarq Biosciences Inc., Canada), anti-mHSP27 (StressMarq Biosciences Inc., Canada), anti-mHSP90alpha (StressMarq Biosciences Inc., Canada), anti-mHSc70(HSP73) (StressMarq Biosciences Inc., Canada), anti-mGRP78 (StressMarq Biosciences Inc., Canada), anti-mHSP90total (StressMarq Biosciences Inc., Canada), anti-mHSP70/HSc70 (StressMarq Biosciences Inc., Canada), anti-mAlpha B crystalline (StressMarq Biosciences Inc., Canada), anti-mHSP70 (StressMarq Biosciences Inc., Canada), anti-mGM-CSF (Pharmigen), anti-mSCA-1 (StressMarq Biosciences Inc., Canada), anti-nitrotyrosine (StressMarq Biosciences Inc., Canada), anti-phospotyrosine (StressMarq Biosciences Inc., Canada), anti-mHSF-1 (StressMarq Biosciences Inc., Canada), and AlexaFluor647 conjugated anti-mIgG (Invitrogen). CellTrace™ Far Red DDAO-SE was purchased from Invitrogen (Carlsbad, CA). The GCSPR/GCSPCF instrument, a dual-mode SPR/Fluorescence instrument, was designed, built and purchased from Ciencia, Inc. (East Hartford, CT).

Mouse Strains
FVB/N female and FVB/N-Tg (MMTV-PyVT)634Mul/J male mice were originally obtained from Jackson Laboratory (Bar Harbor, ME). The control and breast cancer strain are hereafter referred to as FVB and MMTV mice; they were bred and housed in a specified pathogen-free environment with food and water *ad libitum* at The Wadsworth Center. All mice were maintained on a 12-hr light/dark cycle with lights on from 7 AM to 7 PM. Blood samples from the FVB and MMTV mice were collected into EDTA-containing tubes following approved procedures by the Institutional Animal Care and Usage Committee (IACUC) of The Wadsworth Center, NY State

COMMUNICATION

Department of Health (protocol #12-442). MMTV mice with developing tumors were palpated weekly, and the mice were euthanized and bled 12-14 weeks after birth or earlier if tumors became too large.

Antibody Printing

Anti-CD marker and heat shock protein antibodies were initially diluted in PBS buffer (pH 7.4) to working concentration, 0.5 mg/mL, transferred to a 384-well microtiter plate (Thermofisher, IL), and immediately placed in the *Arrayit* robotic microarray spotter, SpotBot II (Arrayit, CA). A total of 85 different antibodies including controls were pin spotted on each 1 cm^2 microchip in triplicate (n= 3 spots or ROIs- Regions of Interest- per analyte), 600 μm apart between each ROI to prevent overlapping, as described below; this was the maximum number of antibodies that could be printed with proper spacing to prevent overlap between each ROI based on the volume per spot.

Microchip Fabrication

In brief, chips were fabricated on 300 mm diameter silicon wafers coated with a 50 nm layer of tetraethyl orthosilicate (TEOS) and a layer of photoresist. Immersion photolithography (193 nm wavelength) was used to pattern the photoresist layer with a sub-micrometer optical SPR grating pattern. Following development of the photoresist, reactive ion etching was used to etch the TEOS layer in the exposed regions, resulting in a three-dimensional grating pattern. Wafers were then diced into 1 cm x 1 cm squares and then coated with titanium (5 nm) and gold (20 nm) using electron beam evaporation.

GCSPR Biosensor Microchips and Microarray Printing

Gold-coated GCSPR biosensor microchips were initially rinsed with 70% ethanol, distilled water and dried under stream of filtered air. The chip was immediately placed in an *Arrayit* robotic microarray spotter, SpotBot II (Arrayit, CA) configured to use one 946MP4 contact pin that has a delivery volume of 1.1 nL and a diameter of 135 μm per spot, and spotted with various anti-mouse antibodies to CD markers, stress proteins, and BSA (essentially globulin-free BSA) (Sigma-Aldrich, St.Louis, MO), which was used as a reference, and goat anti-mouse IgG (0.5 mg/mL). Antibodies were immediately pin spotted in multiples of 3 ROIs per analyte onto the biosensor microchip at room temperature with a relative humidity of 80-90%. After being spotted, the microchip was incubated for 1 hr at room temperature with a relative humidity of 80-90% and stored at 4°C in a desiccator until used.

419 Tumor Cell Line

The 419 MMTV-PyVT mouse model tumor cell line was a kind gift from Dr. Stewart Sell of The Wadsworth Center, NY State Department of Health. Cells were cultured in DMEM medium supplemented with 10% FBS serum (Sigma-Aldrich) and 1% Penicillin-Streptomycin (Sigma-Aldrich), and incubated at 37 °C in a humidified environment of 5% CO_2 in air.

GCSPR Analysis of Blood and 419 Mouse Tumor Cell Line

The printed microchips were assembled at room temperature using a double-sided adhesive gasket (0.50 mm) and a glass window (5 mm) to create a flow cell, 50 μL, and placed in the GCSPR instrument for real-time kinetic binding and fluorescence analysis. At this point, all experiments performed in the instrument were at 32 °C, and all buffer solutions were degassed under vacuum, 25 psi, for 1 hour before use. The microchip was initially washed with freshly degassed PBS buffer (pH 7.4) containing 0.05% Tween 20 for 10 min at a rate of 200 μL/min, blocked with 2% BSA dissolved in PBS buffer for 60 minutes at a flow rate of 200 μL/min, washed for 10 min, and FVB or MMTV mouse blood diluted 1:200 (v/v) with PBS was flowed over the microchip at a rate of 150 μL/min for 60 min. The microchip was then washed a final time for 10 min and real-time kinetic binding data was stored and analyzed.

Experiments involving labeled 419 mouse tumor cells were performed in a similar manner as described above. In brief, 419 cells were labeled with DDAO-SE (Invitrogen C34553) at a concentration of 10 μM at 37 ^{o}C in PBS for 30 minutes following the manufacturer's instructions. The microchip was prepared as described above and 0.1% BSA in PBS was used as a washing buffer. The assembled microchip was initially washed for 10 minutes at a flow rate of 200 μL/min, blocked with 2% BSA at a flow rate of 200 μL/min, and DDAO-SE labeled 419 cells at a concentration of 1 million cells/mL in 0.1% BSA in PBS were flowed over the microchip for 30 min at a rate of 150 μL/min. The microchip was excessively washed a final time for 15 min with 0.1% BSA to remove any non-adherent cells. After the final wash, GCSPCF fluorescence imaging data was collected and analyzed.

MMTV Tumor Single Cell Suspension

Single cell suspensions of breast cancer tumors from the MMTV mice were produced as previously described by Guest *et al*[16]. In brief, MMTV mice with tumors were euthanized following approved IACUC protocols as mentioned above. Tumors were removed from the mice, placed in a small petri dish containing 2 mL of DMEM, cut into small pieces and minced completely with scalpels. The tumor pieces were then placed into a 15 mL Falcon tube containing 3 mg/mL of Collagenase D (Roche) and 3 mg/mL of DNase I (Roche) in 5 mL of DMEM, and the mixture was incubated at 37° C for 10-15 min, dissociated further by pipetting up and down and incubated for an additional 30 min. An equal volume of DMEM with 10% FBS was added and mixed together, followed by filtration of the suspension through a 40 μm nylon mesh (Falcon) and centrifuged at 500 x *g* for 5 min at 4 degrees. The resulting cell pellet was resuspended in DMEM w/ 10% FBS and cells counted using a Coulter-Counter Cell counter. This procedure typically gave a cell count of 2x10^7 cells/mL.

GCSPR Data Processing

The SPR instrument operating software is an executable program written in LabView (National Instruments, Austin, TX). Calculated GCSPR values and GCSPCF fluorescence intensities

represent mean values of 3 ROIs per sample ± standard deviation (SD) performed on Microsoft Excel in which BSA was used as a reference/negative control. Statistical analysis was performed using one-way analysis of variance in which all comparisons of numerical results with a *p* value <0.05 indicates a significant difference.

Results

Mouse 419 mammary derived tumor cells were labeled with CellTrace™ Far Red DDAO-SE as described in the methods section, and real-time binding kinetics were performed using diluted blood from FVB mice or MMTV mice with developing tumors. In order to determine specific surface cell markers most useful for capturing breast cancer cells from blood and evaluating the effectiveness of capturing cells on a microchip, a wide variety of specific and nonspecific antibodies to cell makers were directly spotted on each microchip at a concentration of 0.5 mg/mL. The GCSPR microchip has a nanometer scale three-dimensional pattern on its surface, which is coated with a gold layer. Antibodies spotted on the microchip remain immobilized without covalent crosslinking, allowing the specific detection of cells and/or antigens. It has been well documented that antibodies and proteins adsorb onto gold surfaces through nonspecific electrostatic and hydrophobic interactions[17]. Additionally, serial dilutions of anti-CD44, anti-CD326, anti-CD133 and anti-CD24 were spotted at various locations throughout the microchip in order to optimize the lowest limit of antibody concentration needed for capturing cells and/or antigens.

Initial GCSPR and GCSPCF analysis was performed by using DDAO-SE labeled 419 cells. The 419 cells (10^6/mL) were flowed over a microchip spotted with various anti-CD markers, and captured at regions of interest (ROIs) for specific markers, including CD44, CD326, CD133, CD54, CD49b and CD24 (Fig. 1 and 2). Binding of the 419 cells to the immobilized antibodies was characterized by fluorescence (GCSPCF) and by observing
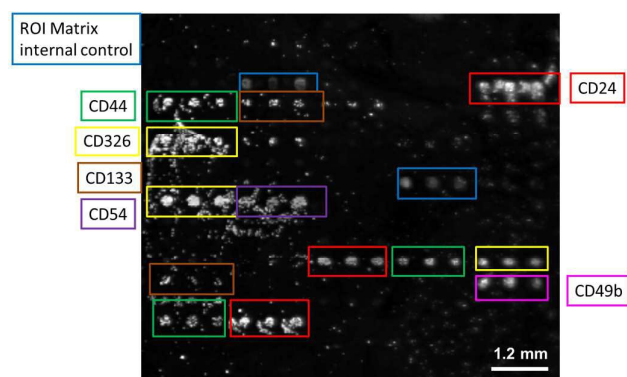
a difference in SPR angle shift from the time buffer was passed over the microchip to the time when the buffer-cell solution was passed over the microchip (Fig. 3). GCSPCF analysis clearly indicates a distinct surface cell marker-antibody binding interaction since mean fluorescence values were obtained for CD44 (203 ± 35), CD24 (219 ± 49), CD133 (87 ± 7), CD326 (229 ± 14), CD152 (58 ± 19), CD38 (25 ± 15), CD54 (111 ± 35), CD71 (33 ± 14), CD49b (121 ± 39) and CD106 (79 ± 20). Corresponding GCSPR angle shifts (mDeg) were also measured for CD24 (90 ± 7), CD44 (81 ± 31), CD133 (58 ± 16), CD326 (118 ± 16), CD49b (73 ± 25), CD71 (16 ± 15) and CD106 (24 ± 18). Additional nonspecific markers spotted on the same microchip bound no cells and/or gave no response (Fig. 4, top).

With the spotting of different concentrations of antibodies that were anticipated to capture the 419 cell line, we assessed the relatively ability of an antibody concentration to capture. As the concentration of the antibody decreased, fewer cells were bound; thus, mean fluorescence intensity decreased, The diluted concentrations of spotted anti-CD44, anti-CD326, anti-CD133 and anti-CD24 throughout the same microchip had different fluorescence intensities, which correlated with the decreasing antibody concentration as fewer cells were captured (Fig. 4, bottom). CD44 spotted at concentrations of 0.2 and 0.1 mg/mL gave GCSPCF mean fluorescence intensities of 133 ± 18, and 78 ± 21, respectively. CD24 spotted at 0.2 mg/mL gave a GCSPCF intensity of 135 ± 28. CD326 spotted at 0.2 mg/mL gave a GCSPCF intensity of 160 ± 36. CD133 spotted at 0.2 mg/mL gave a GCSPCF intensity of 38 ± 34.

To date, most blood tests for CTCs require blood fractionation/separation methods that involve extensive and time-consuming steps[18]. In order to overcome these drawbacks, GCSPR allows for a one-step, label-free procedure with immediate results not involving any fractionation/separation of cells in the blood. This is due to the fact that whole blood can be pumped/flowed across the GCSPR surface, where only cells expressing the correct surface antigens are bound (and immobilized/captured) by antibodies spotted onto the GCSPR chip surface.

Figure 1. GCSPCF image of a microchip in which DDAO-SE labeled 419 mouse tumor cells were captured on antibodies (n= 3 ROIs). Antibodies were spotted throughout the microchip at concentrations ranging from 100 µg/mL to 500 µg/mL. Labeled 419 cells (10^6/mL) were flowed over the microchip for a period of 30 min and non-adherent cells were washed off before GCSPCF imaging.
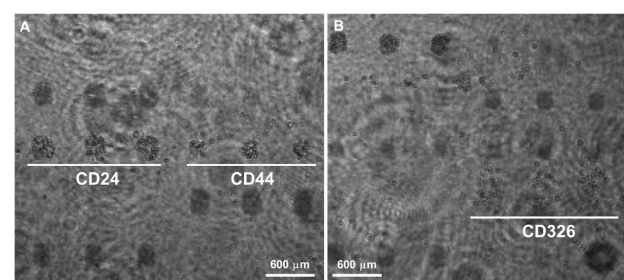

Figure 2. GCSPR ROI image showing DDAO-SE labeled 419 mouse tumor cells captured on (a) CD24 and CD44 ROIs (n=3), and (b) CD326 ROIs (n=3) after the cells (10^6 cells/mL) were flowed over the microchip for a period of 30 minutes. Dark circular patterns on the microchip background showing no cell bound to them are nonspecific antibodies spotted throughout the microchip.
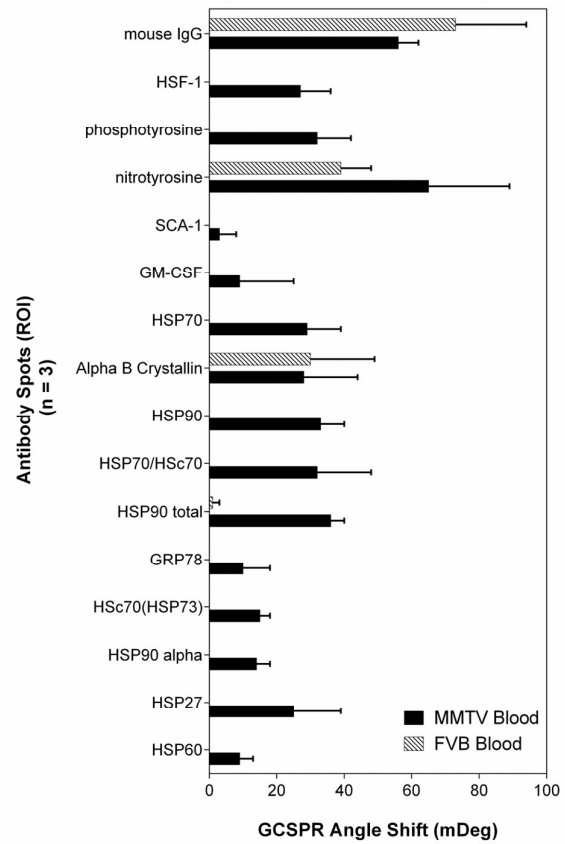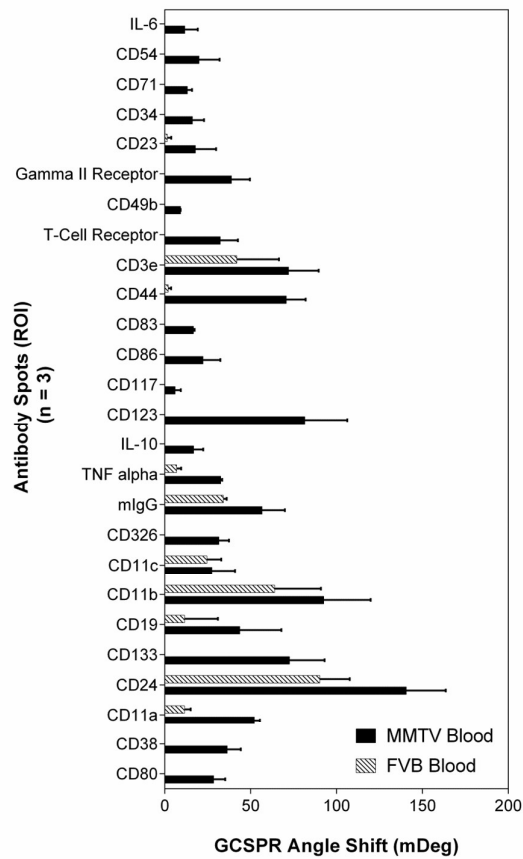
Figure 3. GCSPR real-time binding of 419 cells captured on specific antibodies including CD24 (90 ± 7), CD44 (81 ± 31), CD326 (118 ± 16), CD49b (73 ± 25) and CD133 (58 ± 16). GCSPR binding kinetics began with (a) initial buffer wash of the microchip, followed by blocking with BSA and a wash with buffer, (b) flow of 419 cells (10^6/mL) over the spotted antibodies (n = 3 ROIs) on a microchip and a final wash to remove any non-adherent cells.

In this study, blood from FVB mice (n = 3) or MMTV mice (n = 3) were analyzed with label-free, real-time GCSPR binding kinetics. Diluted blood (1:100 v/v) was flowed over a microchip spotted with various antibodies to tumor cell, leukocyte and plasma protein antigens. The GCSPR characterization of blood (Fig. 5) from MMTV mice compared to FVB mice revealed minimal levels of cells expressing CD117 ($p < 0.04$), CD49b ($p < 0.00001$), IL-6, CD71, CD34 ($p < 0.0000001$), CD83 ($p < 0.00002$), IL-10 ($p < 0.04$), CD23, CD54, and CD86 ($p < 0.02$), moderate levels of cells expressing CD11c, CD80 ($p < 0.004$), CD326 ($p < 0.0008$), T-Cell Receptor ($p < 0.005$), TNF-alpha ($p < 0.006$), CD38 ($p < 0.001$), Gamma II Receptor ($p < 0.006$), CD19, CD11a ($p < 0.0001$), mIgG, and high levels of cells expressing CD44 ($p < 0.004$), CD3ε, CD133 ($p < 0.007$), CD123 ($p < 0.03$), CD11b, and CD24 ($p < 0.01$). Furthermore, since heat shock proteins have long been recognized as target analytes in the early prognosis and detection of breast cancer[19], and since the GCSPR system can simultaneously measure multiple antigen-antibody interactions on the same microchip, various antibodies to heat shock proteins were spotted on each microchip along with the antibodies against surface cell markers. Heat shock proteins HSP60 ($p < 0.02$), HSP27 ($p < 0.04$), HSc70(HSP73) ($p < 0.001$), HSP90 total ($p < 0.001$), HSP70/HSc70 ($p < 0.03$), HSP90 ($p < 0.001$), HSP70 ($p < 0.007$), HSP90 alpha ($p < 0.02$), phosphotyrosine ($p < 0.006$) and HSF-1 ($p < 0.008$) showed a significant difference between MMTV and FVB mice, whereas GRP78, alpha B Crystallin, GM-CSF, SCA-1 and nitrotyrosine did not (Fig. 6).

Figure 4. (Top) GCSPCF analysis of DDAO-SE labeled 419 mouse tumor cells captured on antibodies spotted at a concentration of 500 μg/mL throughout the microchip. Labeled 419 cells (10^6/mL) were flowed over the microchip for a period of 30 minutes and non-adherent cells were washed off. Antibodies having an MFI value <10 were not graphed. GCSPCF analysis of labeled 419 cells captured on antibodies spotted on a microchip at concentrations ranging from 500 μg/mL to 100 μg/mL. Numbers following the antibody represents antibody concentration in μg/mL.

Lastly, GCSPR analysis of a MMTV tumor single cell suspension (10^6 cells/mL) flowed over a microchip spotted with various antibodies indicated a mixture of various cell types and analytes (Fig. 7). Multiple markers gave varying results; however, there was an expression of a few key markers including CD178 (32 ± 8), CD28 (28 ± 6), CXCR4 (12 ± 9), CD197 (9 ± 6), CD11b (65 ± 6), CD14 (42 ± 13), CD62L (27 ± 15), FoxP3 (26 ± 21), CD326 (21 ± 12), CD152 (12 ± 6), CD273 (23 ± 7), IL-10 (6 ± 2), Toll-Like Receptor 2 (8 ± 2), CD71 (16 ± 3), CD31 (11 ± 8), CD127 (36 ± 2), and CD83 (35 ± 18).

Analyst Accepted Manuscript

Figure 5. Real-time GCSPR label-free analysis of diluted (1:100 v/v) blood from FVB (n=3) and MMTV (n=3) mice with tumors. Antibodies (500 µg/mL) were spotted throughout the microchip, and diluted blood was flowed over the microchip for 60 minutes. Binding was assessed by measuring the SPR angle shift caused by changes in the refractive index. Antibodies that gave no signal or showed no significant differences included CD178, CD8, CD5, Early Activation Marker, CD273, Mac-3, mIgG, CD28, IFN gamma, CD25, CD26, IL-12, CXCL12/SDF1, CXCR4, CD4, CD197, CD49f, CD152, CD40, CD138, CD14, CD31, CD45, CD90.2, FoxP3, Annexin V and CD69 were not graphed.

Figure 6. Real-time GCSPR label-free analysis of heat shock proteins from blood and/or cells of FVB and MMTV mice. HSPs were spotted along with various makers throughout the microchip at concentrations of 500 µg/mL. GCSPR binding analysis was performed simultaneously along with the antibodies in Figure 3. Blood was flowed over the microchip for a period of 60 minutes and binding was determined by measuring changes in the refractive index.

Analyst Accepted Manuscript
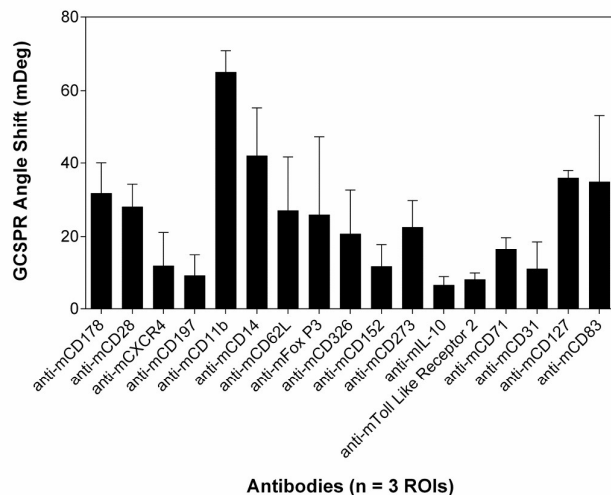
Figure 7. Real-time, label-free GCSPR analysis of a MMTV mouse tumor single cell suspension. Antibodies were spotted throughout a microchip at concentration of 500 μg/mL. The single cell suspension (10^7 cells/mL) was flowed over the microchip for a period of 60 minutes and binding was determined by observing changes in the refractive index.

Discussion

Microfluidic devices or lab-on-a-chip (LOC) technologies have a wide range of medical applications and have been the topic of much research[20]. The focus of these technologies is centered on the need for early assessment of a developing diseases as well as the ability to provide a prognostic indicator. However, the biggest limitation of current technologies has been the limited number of analytes that can be measured at a time, which prevents developing a complete immune profile of the host. Understanding the host's immune status, physical/psychological condition and stress level is of importance, especially with regard to the presence of a cancer. Current medical diagnostics applicable to CTC detection rely on labeling of CTCs with antibodies conjugated to magnetic particles and characterization by immunofluorescence or RT-PCR at the RNA level[21]. There is, however, no simultaneous analysis of the host's response or expression of any secreted tumor cell products.

One developing technology, surface plasmon resonance (SPR) based biosensors, which offer the ability to measure real-time binding interactions under continuous flow conditions, are ideal tools for detecting analytes from complex samples[19]. Herein, we have described the use of a dual-mode, grating-coupled SPR-based instrument[13] capable of real-time, label-free measurements (GCSPR) and fluorescence (GCSPCF) imaging to increase sensitivity using a gold-coated grating-based microchip for the detection of CTCs. GCSPR and GCSPCF

imaging circumvents the above mentioned limitations by using small quantities of detection/capture antibodies to detect multiple types of analytes such as CTCs and their secreted products, tumor specific antigens (TSAs) and plasma antibodies, cytokines, peripheral blood leukocytes, and stress proteins, which allows for a more complete immune profile of the host in the presence of cancer or expression of factors associated with tumor growth and/or immune response against the tumor.

Our preliminary GCSPR and GCSPCF data obtained using labeled 419 cells demonstrated the ability to capture cells at ROIs. The 419 cells were captured from solution and bound to the immobilized antibodies, which were spotted directly onto the gold-coated microchip. Binding was characterized by fluorescence, and by observing a difference in the SPR angle shift[13]. A change in the local refractive index (RI) due to association of biological molecules, cells, etc. is what causes a shift in the GCSPR angle and therefore the measurable signal. Thus, the observed shift in SPR angle is due to the RI changes at ROIs of antibodies spotted on the biosensor surface, in addition to the effective thickness increase of the adsorbed cell layer, while the critical angle remains fixed[13]. Therefore, at a greater antibody concentration, there is additional binding between the antibody and 419 cells. Hence, the effective thickness of the adsorbed cell layer, when equilibrium is achieved, is related to the concentration of the antibody and the stoichiometry of the antibody and the captured molecule/particle. Overall, strong binding interactions are reflective of positive SPR angle shifts whereas weak or no binding is reflective of little, if any, SPR angle shifts[22].

Breast cancer develops aggressively in female MMTV mice; thus, these mice possess an enhanced metastatic potential in which blood can be used to evaluate host responses that measure differences in immune, neuroendocrine and stress-related factors. The direct detection and characterization of CTCs in blood from MMTV mice remains difficult. The degree of binding and SPR angle shift gets more complicated when running whole blood samples, since blood has multiple components (red blood cells, white blood cells, platelets, plasma). Matrix proteins from blood appear to inhibit the binding of antigens at low antibody concentrations immobilized on the biosensor surface. Thus, our GCSPR results were solely based on antibodies spotted at a concentration of 500 μg/mL. The lack of binding at low antibody concentrations may indicate a saturation of available binding sites of the antibody or it could be that the antibody binding sites form either weak binding interactions or don't bind at all because of steric crowding by matrix proteins.

In capturing labeled 419 cells on a microchip, a few suitable markers including CD326 (EpCAM), CD49b, CD133, CD24 and CD44 were found. However, in blood samples from MMTV mice with developing tumors, CD326 was the ideal marker for detecting circulating and metastasizing cancer cells. CD326 is a well-known tumor-associated antigen expressed in a variety of cancers[23]. Other markers, including CD34 and CD133, were also important. CD133 alone can be used as a marker for profiling breast cancer[24] whereas CD34 is an endothelial cell marker used as an angiogenic marker for tumor growth[25] and a stem cell marker for many cancer progenitors. CD24 and CD44 were also suitable for capturing 419 cells; however, capturing CTCs in the presence of blood or any soluble tumor-specific antigens (TSAs) or erythrocytes is complicated since blood has multiple components. Furthermore, erythrocytes are known to maintain high levels of CD24, and expression of CD24 by other nonmalignant cell types is also common[26].

The expression of CD326 (EpCAM) in blood samples from MMTV mice correlates with previously published reports in which CD326 was over-expressed in a variety of cancers including lung, prostate, and breast cancer[27, 28]. Similarly, the elevated expression of CD34, CD38 and CD133 was noticeable in blood from MMTV mice suggesting, to some extent, that this was mediated by developing tumors[24, 29]. Interestingly, there was an expression of IL-10 in MMTV mice compared to FVB mice. This, of course, adds to the ongoing debate associated with IL-10 and its role associated with tumor progression[30, 31]. It is well documented that cytokines such as IL-6, IL-10 and tumor necrosis factor-α (TNF-α) play a key role in regulating immune responses[32]; however, different cytokines can either promote or inhibit tumor promotion and development[33] as well as produce detrimental processes such as angiogenesis, metastasis, and anti-apoptotic effects, which lead to tumor promotion[34-36]. The expression of CD11a, CD11b, CD11c, CD54, CD71, CD80, CD83 and CD123 seems to be associated with dendritic cells (DCs), dendritic cell immune response and/or activated T and B cells due to the developing tumors[37-42].

The overexpression of heat shock proteins in a wide number of cancers, and their use as biomarkers for carcinogenesis, has previously been reported[43]. It is also well known that HSPs are overexpressed in mammary carcinoma cells[44]. The significant differences found with HSP60, HSP27, HSc70(HSP73), GRP78, HSP90 total, HSP70/HSc70, HSP90, HSP70, phosphotyrosine and HSF-1 between MMTV and FBV mice further validates these reports. For example, HSc70 has been overexpressed and plays a role in wide spectrum of cancer cells[45]. GRP78 has been reported to be upregulated in various cancers since cancer cells proliferate at a high rate and require increased protein synthesis[46, 47]. Additional HSPs have been implicated with the prognosis of specific cancers, most notably HSP27[48], whose expression is associated with mammary tumors and cancer cell growth, and HSP70[49], which is correlated with poor prognosis in breast carcinomas. Implication of HSP90 in tumor progression is questionable since it's an abundant protein in

cells and is stimulated by stress; however, high levels of HSP90 and HSP transcriptional factor 1 (HSF-1) have been reported to be correlated with the poor prognosis of breast cancer subtypes[50]. Lastly, HSP60 has been known to be expressed in tumor cells[51] whereas phosphotyrosine was identified in breast cancer cells[52].

Lastly, we found no additional binding or shifts in the SPR angle when an MMTV tumor single cell suspension was flowed over a microchip after pre-treatment of the chip with a whole blood sample (data not shown). There was either no binding or there was interference from the mass of adsorbed proteins onto the biosensor surface. As previously mentioned, blood has many components, and it could be that antibody binding sites were saturated. Therefore, at low antigen concentrations, the binding of antigens to the antibody immobilized on the biosensor surface is limited. In order to assure binding of antigens at low concentrations to antibodies without interference from matrix proteins, we have developed a bump-array device incorporating GCSPR that addresses this issue[53]. In essence, the bump-array device separates blood components (plasma, platelets, red blood cells, leukocytes, and CTCs) prior to their exposure to the GCSPR chip. This is hypothesized to limit the interference of freely soluble antigens/cell surface markers with antibody-based capture of target cells.

Conclusions

In conclusion, the GCSPR and GCSPCF imaging microarray presented above provides a versatile, easy-to-use, rapid and inexpensive immunoassay for screening blood for various analytes. Our focus was on screening blood from MMTV mice for CTCs; however, screening for multiple analytes including cytokines, leukocytes, plasma antibodies and heat shock proteins was also performed simultaneously on the same microchip. No other current technology is capable of performing simultaneous, multiplex analysis of a wide range of components. This microarray offers a direct, label-free platform for screening analytes requiring little to no sample preparation. Thus, our broad-spectrum analysis of factors considerably provides more information that can be used for diagnosis/prognosis since we assessed the immunological, inflammatory, and cellular and systemic stress responses that are profiled in the host, MMTV mice, with developing mammary tumors.

Acknowledgements

COMMUNICATION

References

1. R. Nadal, J. A. Lorente, R. Rosell and M. J. Serrano, *Expert Rev Mol Diagn*, 2013, **13**, 295-307.

2. K. Pantel and C. Alix-Panabieres, *J Thorac Dis*, 2012, **4**, 446-447.

3. M. Balic, H. Lin, A. Williams, R. H. Datar and R. J. Cote, *Expert Rev Mol Diagn*, 2012, **12**, 303-312.

4. S. Zheng, H. K. Lin, B. Lu, A. Williams, R. Datar, R. J. Cote and Y. C. Tai, *Biomed Microdevices*, 2011, **13**, 203-213.

5. R. Nadal, A. Fernandez, P. Sanchez-Rovira, M. Salido, M. Rodriguez, J. L. Garcia-Puche, M. Macia, J. M. Corominas, M. Delgado-Rodriguez, L. Gonzalez, J. Albanell, M. Fernandez, F. Sole, J. A. Lorente and M. J. Serrano, *Breast Cancer Res*, 2012, **14**, R71.

6. G. Somlo, S. K. Lau, P. Frankel, H. B. Hsieh, X. Liu, L. Yang, R. Krivacic and R. H. Bruce, *Breast Cancer Res Treat*, 2011, **128**, 155-163.

7. C. T. Guy, R. D. Cardiff and W. J. Muller, *Mol Cell Biol*, 1992, **12**, 954-961.

8. A. Fantozzi and G. Christofori, *Breast Cancer Res*, 2006, **8**, 212.

9. M. Cristofanilli, G. T. Budd, M. J. Ellis, A. Stopeck, J. Matera, M. C. Miller, J. M. Reuben, G. V. Doyle, W. J. Allard, L. W. Terstappen and D. F. Hayes, *N Engl J Med*, 2004, **351**, 781-791.

10. www.cancer.gov

11. www.nationalbreastcancer.org

12. G. B. Jin, D. W. Unfricht, S. M. Fernandez and M. A. Lynes, *Biosens Bioelectron*, 2006, **22**, 200-206.

13. D. W. Unfricht, S. L. Colpitts, S. M. Fernandez and M. A. Lynes, *Proteomics*, 2005, **5**, 4432-4442.

14. D. G. Lanza, J. Ma, I. Guest, C. Uk-Lim, A. Glinskii, G. Glinsky and S. Sell, *Tumour Biol*, 2012, **33**, 1997-2005.

15. J. Ma, D. G. Lanza, I. Guest, C. Uk-Lim, A. Glinskii, G. Glinsky and S. Sell, *Tumour Biol*, 2012, **33**, 1983-1996.

16. I. Guest, Z. Ilic and J. Ma, in *Curr Protoc Toxicol*, 2011/11/08 edn., 2011, vol. Chapter 22, p. Unit22 23.

17. E. E. Ferapontova, V. G. Grigorenko, A. M. Egorov, T. Borchers, T. Ruzgas and L. Gorton, *Biosens Bioelectron*, 2001, **16**, 147-157.

18. Z. A. Nima, M. Mahmood, Y. Xu, T. Mustafa, F. Watanabe, D. A. Nedosekin, M. A. Juratli, T. Fahmi, E. I. Galanzha, J. P. Nolan, A. G. Basnakian, V. P. Zharov and A. S. Biris, *Sci Rep*, 2014, **4**, 4752.

19. L. S. Kim and J. H. Kim, *J Breast Cancer*, 2011, **14**, 167-174.

20. E. Helmerhorst, D. J. Chandler, M. Nussio and C. D. Mamotte, *Clin Biochem Rev*, 2012, **33**, 161-173.

21. N. Krawczyk, F. Meier-Stiegen, M. Banys, H. Neubauer, E. Ruckhaeberle and T. Fehm, *Biomed Res Int*, 2014, **2014**, 415721.

22. V. Yashunsky, V. Lirtsman, M. Golosovsky, D. Davidov and B. Aroeti, *Biophys J*, 2010, **99**, 4028-4036.

23. P. A. Baeuerle and O. Gires, *Br J Cancer*, 2007, **96**, 417-423.

24. G. Furstenberger, R. von Moos, R. Lucas, B. Thurlimann, H. J. Senn, J. Hamacher and E. M. Boneberg, *Br J Cancer*, 2006, **94**, 524-531.

25. L. T. Mikalsen, H. P. Dhakal, O. S. Bruland, J. M. Nesland and D. R. Olsen, *Anticancer Res*, 2011, **31**, 4053-4060.

26. B. Li, Q. Shao, D. Ji, F. Li, X. Guo and G. Chen, *Diagn Pathol*, 2014, **9**, 209.

27. R. Konigsberg, E. Obermayr, G. Bises, G. Pfeiler, M. Gneist, F. Wrba, M. de Santis, R. Zeillinger, M. Hudec and C. Dittrich, *Acta Oncol*, 2011, **50**, 700-710.

28. M. Trzpis, P. M. McLaughlin, L. M. de Leij and M. C. Harmsen, *Am J Pathol*, 2007, **171**, 386-395.

29. F. Karimi-Busheri, A. Rasouli-Nia, V. Zadorozhny and H. Fakhrai, *Multidiscip Respir Med*, 2013, **8**, 65.

30. L. Giordani, P. Bruzzi, C. Lasalandra, M. Quaranta, F. Schittulli, F. Della Ragione and A. Iolascon, *Clin Chem*, 2003, **49**, 1664-1667.

31. W. W. Sung and H. Lee, *Oncoimmunology*, 2013, **2**, e25854.

32. V. S. Rao, C. E. Dyer, J. K. Jameel, P. J. Drew and J. Greenman, *Oncol Rep*, 2006, **15**, 179-185.

33. B. F. Zamarron and W. Chen, *Int J Biol Sci*, 2011, **7**, 651-658.

34. S. I. Grivennikov, F. R. Greten and M. Karin, *Cell*, 2010, **140**, 883-899.

35. M. Moreno-Smith, S. K. Lutgendorf and A. K. Sood, *Future Oncol*, 2010, **6**, 1863-1881.

36. H. A. Smith and Y. Kang, *J Mol Med (Berl)*, 2013, **91**, 411-429.

37. T. Boettler, E. Panther, B. Bengsch, N. Nazarova, H. C. Spangenberg, H. E. Blum and R. Thimme, *J Virol*, 2006, **80**, 3532-3540.

38. M. F. Lipscomb and B. J. Masten, *Physiol Rev*, 2002, **82**, 97-130.

39. D. F. Miranda-Hernandez, M. A. Franco-Molina, E. Mendoza-Gamboa, P. Zapata-Benavides, C. A. Sierra-Rivera, E. E. Coronado-Cerda, A. G. Rosas-Taraco, R. S. Tamez-Guerra and C. Rodriguez-Padilla, *Oncol Lett*, 2013, **6**, 1195-1200.

40. S. R. Ross, J. J. Schofield, C. J. Farr and M. Bucan, *Proc Natl Acad Sci U S A*, 2002, **99**, 12386-12390.

41. U. Testa, E. Pelosi and A. Frankel, *Biomark Res*, 2014, **2**, 4.

42. M. Wolenski, S. O. Cramer, S. Ehrlich, C. Steeg, G. Grossschupff, K. Tenner-Racz, P. Racz, B. Fleischer and A. von Bonin, *Med Microbiol Immunol*, 2003, **192**, 189-192.

43. G. Jego, A. Hazoume, R. Seigneuric and C. Garrido, *Cancer Lett*, 2013, **332**, 275-285.

44. S. K. Calderwood and J. Gong, *J Cell Biochem*, 2012, **113**, 1096-1103.

45. P. Nirde, D. Derocq, M. Maynadier, M. Chambon, I. Basile, M. Gary-Bobo and M. Garcia, *Oncogene*, 2010, **29**, 117-127.

46. D. Dong, M. Ni, J. Li, S. Xiong, W. Ye, J. J. Virrey, C. Mao, R. Ye, M. Wang, L. Pen, L. Dubeau, S. Groshen, F. M. Hofman and A. S. Lee, *Cancer Res*, 2008, **68**, 498-505.

47. B. Luo and A. S. Lee, *Oncogene*, 2013, **32**, 805-818.

48. W. Porter, F. Wang, R. Duan, C. Qin, E. Castro-Rivera, K. Kim and S. Safe, *J Mol Endocrinol*, 2001, **26**, 31-42.

49. S. K. Calderwood, *Int J Hyperthermia*, 2010, **26**, 681-685.

50. Q. Cheng, J. T. Chang, J. Geradts, L. M. Neckers, T. Haystead, N. L. Spector and H. K. Lyerly, *Breast Cancer Res*, 2012, **14**, R62.

51. F. Cappello, E. Conway de Macario, L. Marasa, G. Zummo and A. J. Macario, *Cancer Biol Ther*, 2008, **7**, 801-809.

52. E. E. Lower, M. A. Miller, L. Williams, C. Westermann and S. Heffelfinger, *Breast Cancer Res Treat*, 1995, **35**, 277-282.
53. J. S. Holt, A. Mendoza, D. Lawrence and N. C. Cady, *MRS Online Proceedings Library*, 2014, **1686**, null-null.